Biophysical Journal, Volume *110*

Supplemental Information

Oligomerization of the Tetraspanin CD81 via the Flexibility of Its δ-Loop

Thomas H. Schmidt, Yahya Homsi, and Thorsten Lang

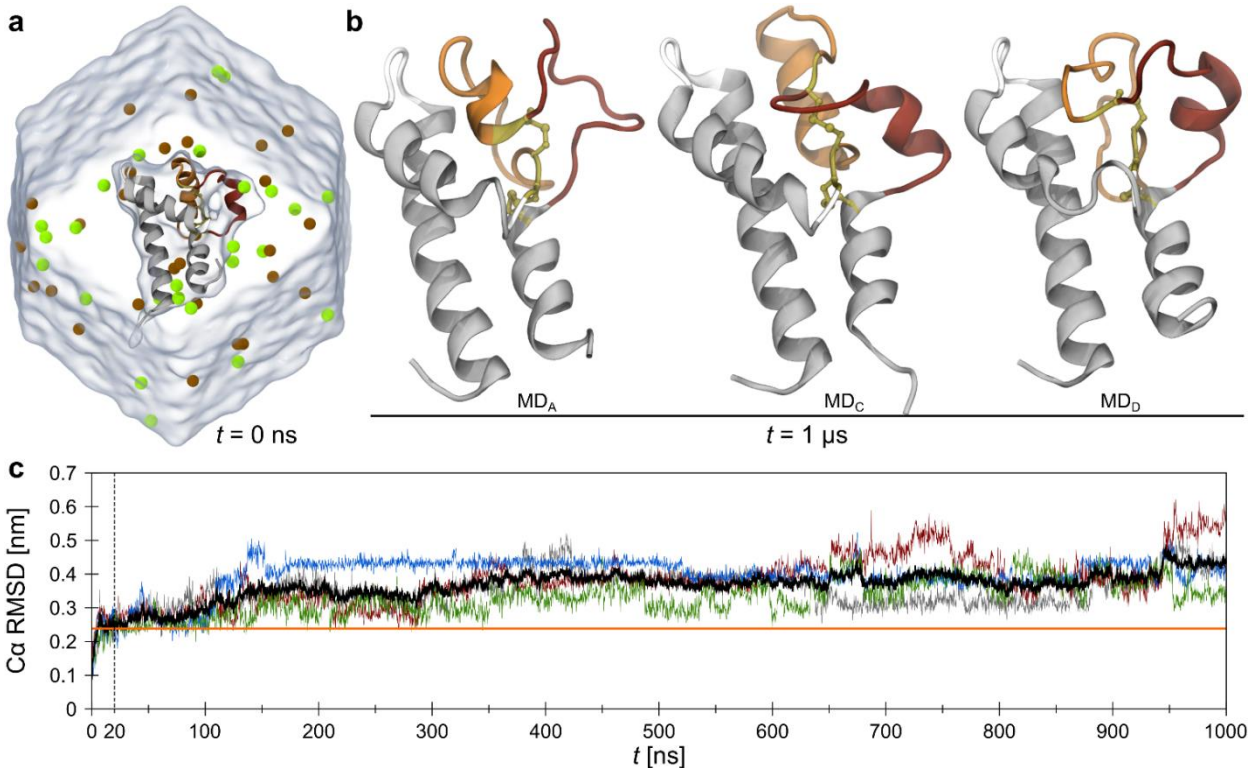

Fig. S1. Initial MD simulation system and final conformations of $CD81_{LEL}$.
a) MD initial configuration of the $CD81_{LEL}$ system. The energy minimized $CD81_{LEL}$ structure was placed in the center of the simulation box (rhombic dodecahedron), which was filled up by a 150 mM NaCl solution. For clarity, the aqueous phase is represented as semi-transparent volume surface, Na^+ and Cl^- ions are colored in tan and green, respectively. b) $CD81_{LEL}$ conformations after 1 µs unbiased simulation of run A, C, and D (for the final conformation of run B see Fig. 1a). The γ- and δ-loops are shown in orange and red, respectively. c) Cα root mean square deviation (RMSD) as a function of time, after least-square fitting to the MD initial structure. Grey, green, blue, and red indicate individual MD runs; the average is shown in black (n = 4). The orange reference line indicates 50% change (reached after ≈20 ns) with reference to the average RMSD maximum.

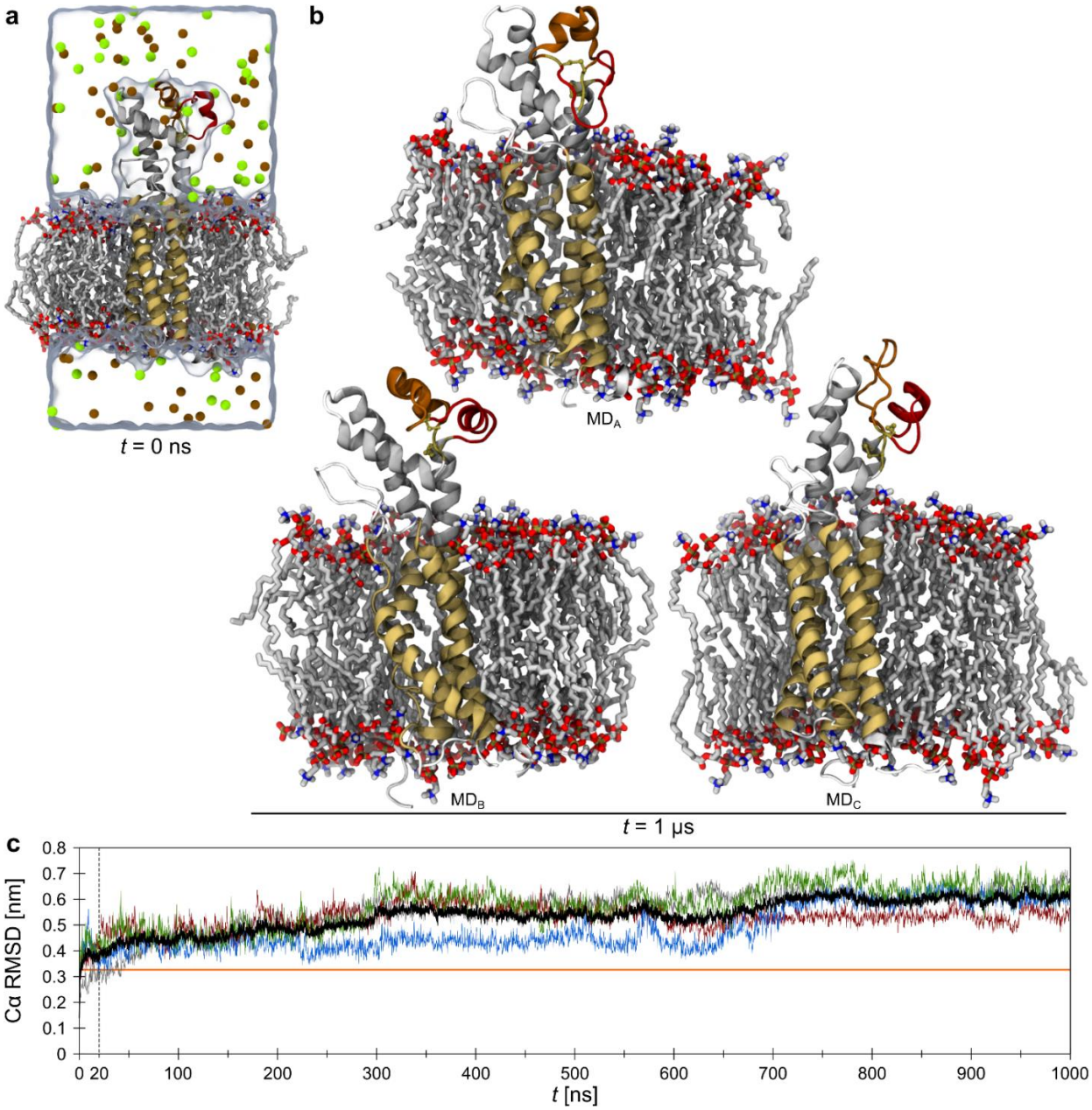

Fig. S2. Initial MD simulation system and final conformations of $CD81_{FL}$.
a) MD initial configuration of the $CD81_{FL}$ system. The energy minimized $CD81_{FL}$ structure was embedded into a POPC lipid bilayer. Then the simulation box was filled up with a 150 mM NaCl solution. For clarity, the aqueous phase is shown as semi-transparent volume surface, with Na^+ and Cl^- ions in tan and green, respectively. b) $CD81_{FL}$ conformations after 1 µs unbiased simulation of run A, B, and C (for the final conformation of run D see Fig. 2a). The γ-loop, δ-loop and transmembrane helices are shown in orange, red and yellow, respectively. Foreground POPC lipids were hidden to illustrate the embedded protein. c) Cα RMSD with reference to the MD initial structure as a function of time. Grey, green, blue, and red show individual MD runs; the average is shown in black (n = 4). The orange reference line indicates 50% change (reached after ≈20 ns) with reference to the average RMSD maximum.

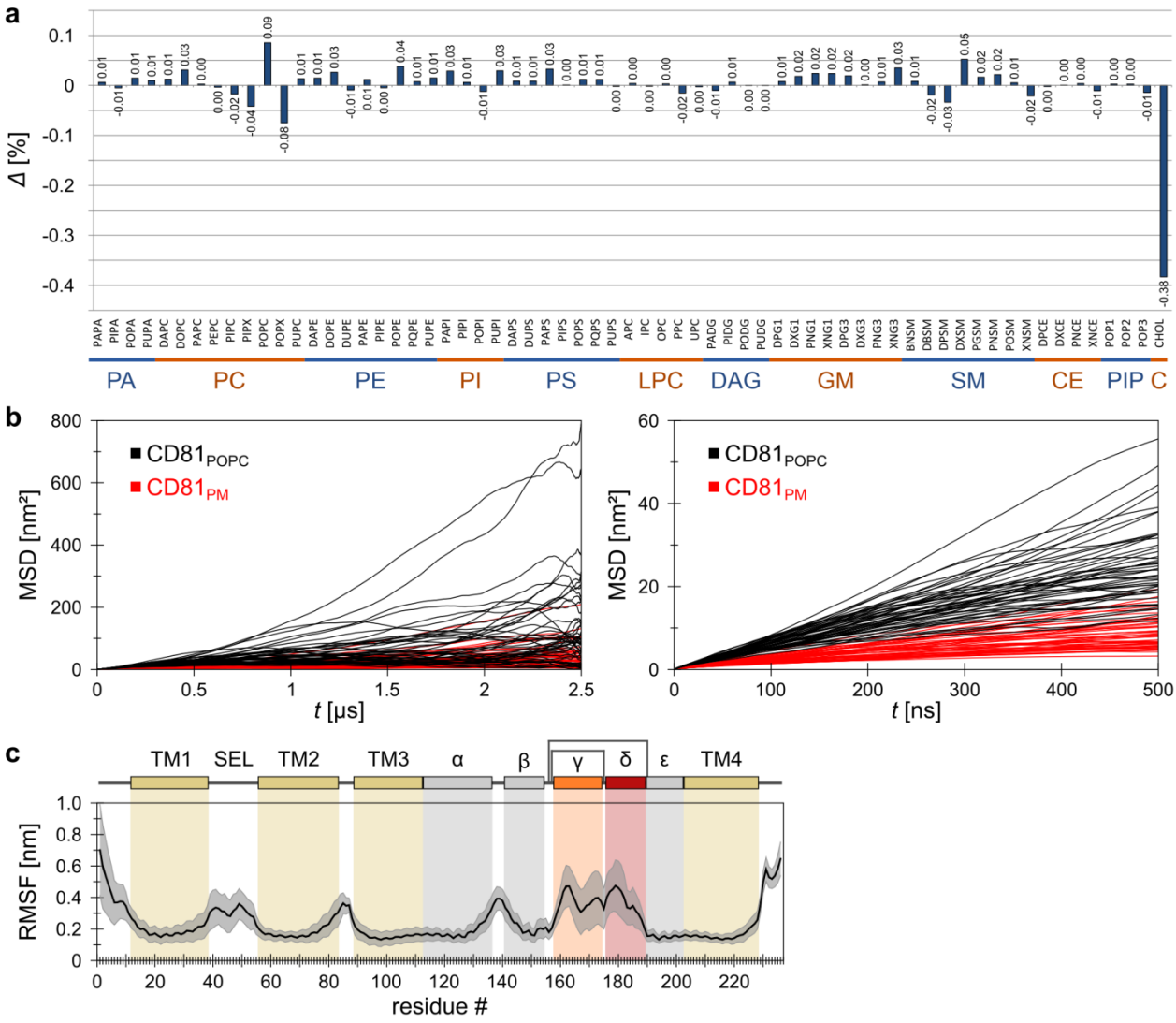

Fig. S3. Change of lipid composition after protein embedding and CD81 dynamics in the plasma membrane.

a) During membrane protein embedding, a certain number of protein-overlapping lipids were deleted from the plasma membrane patch, generating differences *Δ* (in percent) to the original plasma membrane lipid composition (1). Lipid species are grouped by type/head group to phosphatidic acid (PA), phosphatidylcholine (PC), phosphatidylethanolamine (PE), phosphatidylinositol (PI), phosphatidylserine (PS), lysophosphatidylcholine (LPC), diacylglycerol (DAG), ganglioside (GM), sphingomyelin (SM), ceramide (CE), phosphatidylinositol (mono/bis/tris)-phosphate (PIP), and cholesterol (C; in Fig. S4 referred to as CHOL). For the exact description of the different lipids within each group please refer to (1).

b) Mean squared displacement (MSD) plotted versus time (left shows the entire analysis, right the first 500 ns) for individual CD81 proteins embedded in the plasma membrane (red traces) or in the POPC bilayer (black traces). c) RMSF for CD81 in the plasma membrane system.

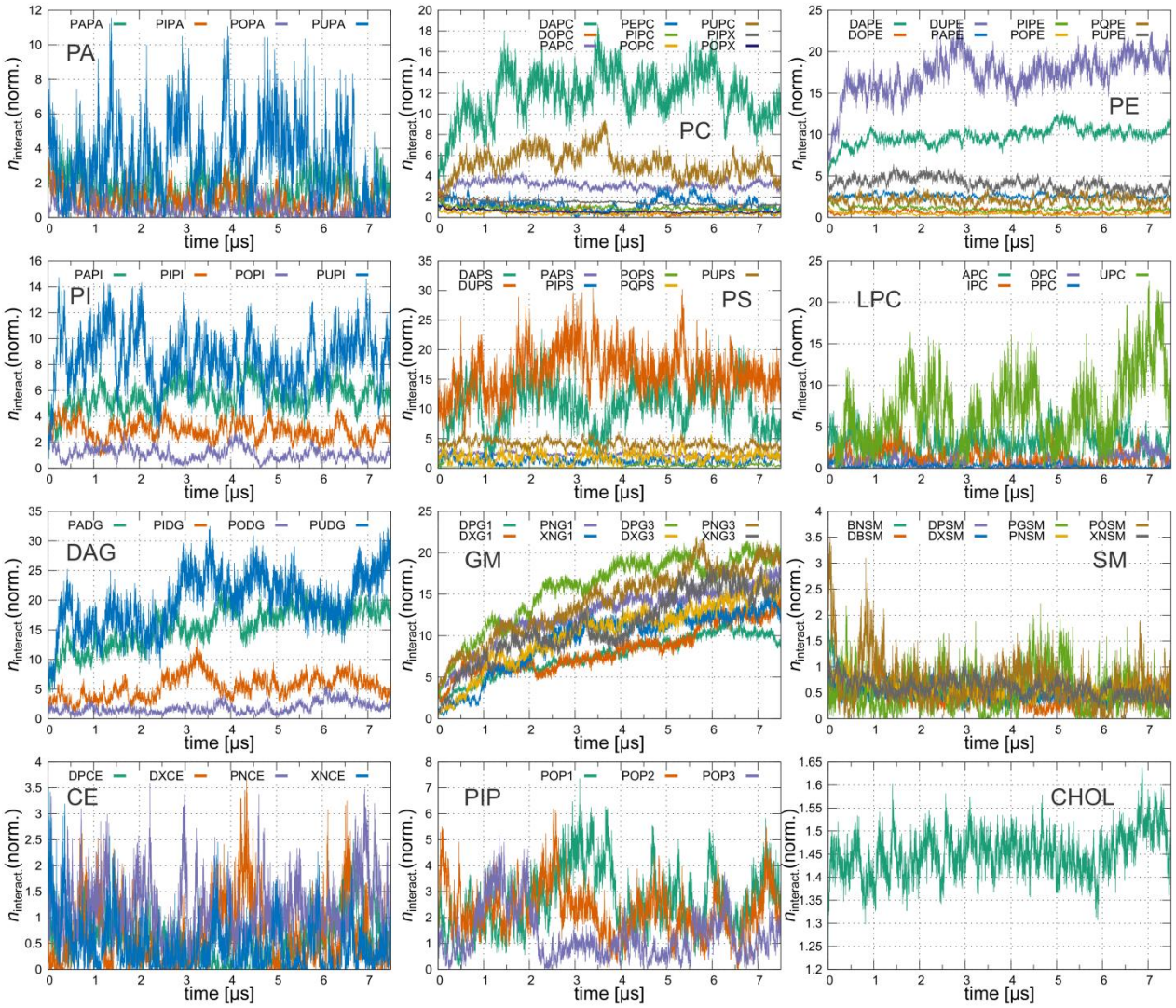

Fig. S4. Number of CD81 interactions with different lipid species.
Number of contacts between CD81 molecules and the individual lipid species (for abbreviations see Fig. S3) as function of time. Contacts were normalized to the concentration of the respective lipid type. Normalization shows that some low-concentrated lipids, e.g. the PC species DAPC, increase their contacts over time while the PC type POPX shows a trend to diminished binding. Because POPX is much more abundant than DAPC, it dominates the trace summing up all contacts between CD81 and PC (Fig. 6d). Notably, in the case of GM, irrespective of the concentration, all GM species show increased contacts over time.

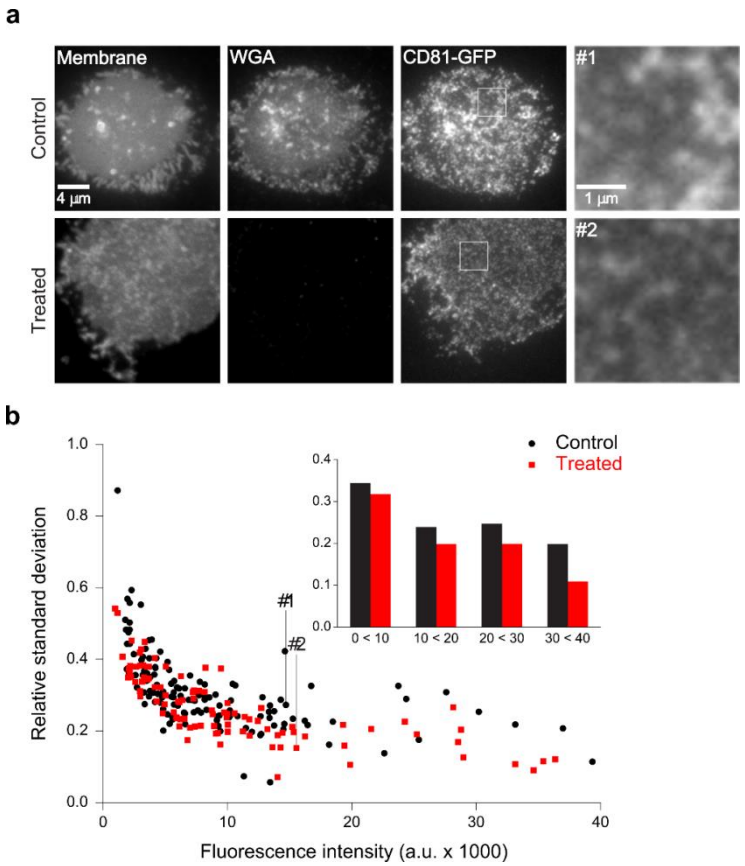

Fig. S5. Degradation of the glycocalyx disperses CD81 domains.
a) Membrane sheets from Jurkat T cells expressing GFP-labelled CD81 for the visualization of CD81 domains. Prior to membrane sheet generation, cells were treated without (control) or with (treated) neuraminidase and β-galactosidase (for which gangliosides are a substrate). Left to right, membrane visualized by TMA-DPH (showing the integrity of the membrane), staining for sialic acid and *N*-acetyl-glucosaminyl residues by the lectin WGA coupled to Alexa Fluor® 594, and CD81 domains (CD81-GFP) as overview and magnified views (indicated by the white squares in the overview). Images in the red and green channels have the same scaling, respectively. Enzymes treatment reduces WGA staining to 39.6 ± 8.1% (n = 3 independent experiments; for each experiment 37 - 122 membrane sheets from untransfected and transfected cells were analyzed). CD81-GFP signal intensity in the control and the treated membrane (showing almost no WGA staining) were similar (see also (b)) but signal in the control is concentrated in brighter spots. b) For a representative illustration, the relative standard deviation (rel. S.D.) was determined which allows for comparison of the inhomogeneity of similarly intense signals. The rel. S.D. from individual membranes was plotted against the CD81-GFP intensity (black, control; red, enzyme treated). Data points from three independent experiments were pooled (20 - 58 membrane sheets per day and condition; highest expression levels were all from one day). For better comparison, the inset shows a histogram of the averaged rel. S.D. at expression levels binned at 10,000 a.u. steps. The dispersion effect is small because the remaining ≈40% may be sufficient to maintain indirect patching. In the graph the two membranes shown in (a) are marked with #1 and #2.

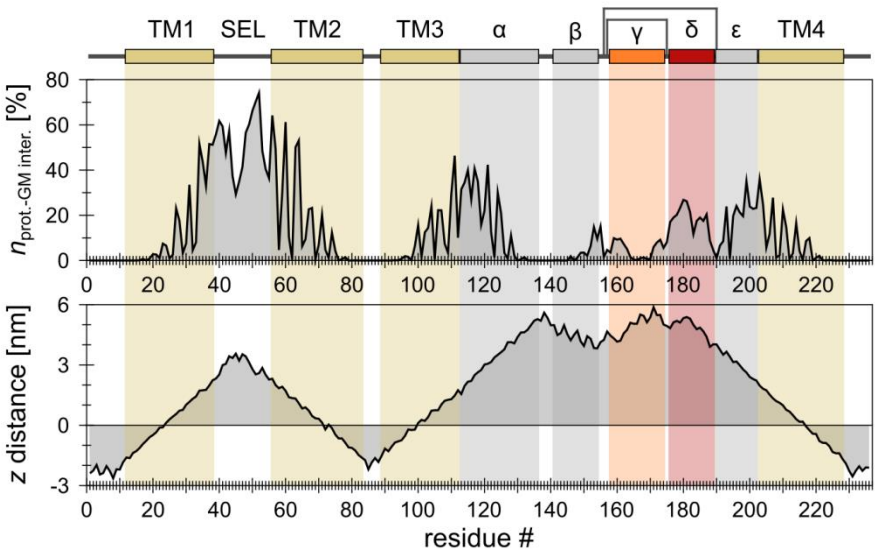

Fig. S6. CD81-GM1 interacting residues and their distance to the membrane.
Top, protein-ganglioside (GM) interactions as a function of residue in percent. Bottom, z-distance of the individual residues (center of mass) to the hydrophobic belt center (set to zero) in the atomistic MD starting configuration. Protein orientation and hydrophobic belt detection were performed by the program LAMBADA. For Fig. 6e values from the top graph were multiplied with the values from the lower graph.

SUPPORTING REFERENCE

1. Ingólfsson, H.I., M.N. Melo, F.J. van Eerden, C. Arnarez, C.A. Lopez, T.A. Wassenaar, X. Periole, A.H. de Vries, D.P. Tieleman, and S.J. Marrink. 2014. Lipid Organization of the Plasma Membrane. J. Am. Chem. Soc. 136: 14554–14559.